EFFECT OF SECONDARY ELECTRON EMISSION COEFFICIENT ON TOWNSEND'S SECOND IONISATION COEFFICIENT

TOMOKAZU YOSHINAGA AND HARUAKI AKASHI

Department of Applied Physics, National Defense Academy, Yokosuka, 239-8686, Japan
Corresponding author's e-mail: yoshinag@nda.ac.jp

ABSTRACT

To clarify the relationship between secondary electron emission coefficient and secondary ionisation coefficient, Ar dielectric barrier discharges have been simulated using one dimensional fluid model. The Paschen's curves are obtained and secondary ionisation coefficients are derived from the Townsend's breakdown criterion. Each secondary electron emission coefficients affect to breakdown voltages and secondary ionisation coefficients. However, it is found that the secondary ionisation coefficients are obtained in similar to that of secondary electron emission coefficients.

1. INTRODUCTION

Secondary electron emission coefficients play an important role in recent plasma applications, on the other hand, it is known as one of the confusing coefficients. Generally secondary electron emission coefficient is notated as γ, and secondary ionisation coefficient (Townsend's second ionisation coefficient) is also notated as γ.

Recently dielectric barrier discharges (DBDs) have been applied on many fields and it is known that the secondary electron emission coefficients affect DBDs significantly. However, the coefficient of dielectrics is mostly unknown, except the coefficients might be higher than that of metal electrodes. There are some difficulties to measure the coefficients, such as accumulation of charges on the surface of dielectrics. G. Auday et al[1] and S. Suzuki et al[2] have tried to measure the coefficient of MgO. But it is very difficult to measure it, then, they have measured the secondary ionisation coefficient. It is important to know the values of the coefficient, because the coefficients are assumed to have a close relationship with secondary electron emission coefficients (SEE coeeficients). But the relationship is not clarified, yet. So if the relationship is found, many accurate secondary electron emission coefficients are obtained. In this paper, using a simple one dimensional fluid model, relation between the secondary electron emission coefficient and secondary ionisation coefficient has been investigated.

2. MODELLING

Discharges between the two parallel plane electrodes are modelled as shown in Fig. 1. The dielectric barrier with relative permittivity ε_r of 4.7 and its thickness b of 0.1 cm is set on the grounded electrode surface. The gap distance d is 0.2cm. The discharge column is assumed with cross section S of 4cm^2. As modelled in one dimension, discharge parameters only vary with the distance from the barrier surface. As an external circuit, a capacitor C (=20nF) is connected on the grounded electrode and a resistor R (=500kΩ) on the powered electrode. The sinusoidal voltage with amplitude at 500V and frequency f of 20 Hz is applied. The background gas pressure p_0 is changed from 1–100Torr and 0◦C is assumed for the gas temperature. In the present model, five species are considered, electron, positive ion (Ar^+), positive dimer ion (Ar_2^+), metastable state atom (Ar^{ms}) and other excited atom (Ar^{ex}). And the

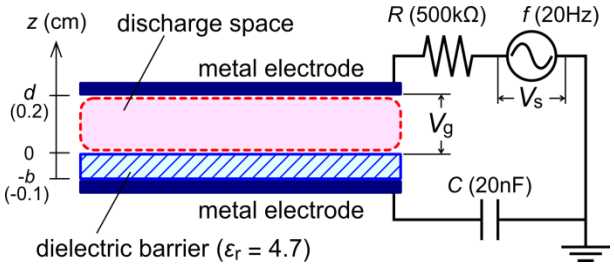

Fig. 1. Model configuration for the present simulation.

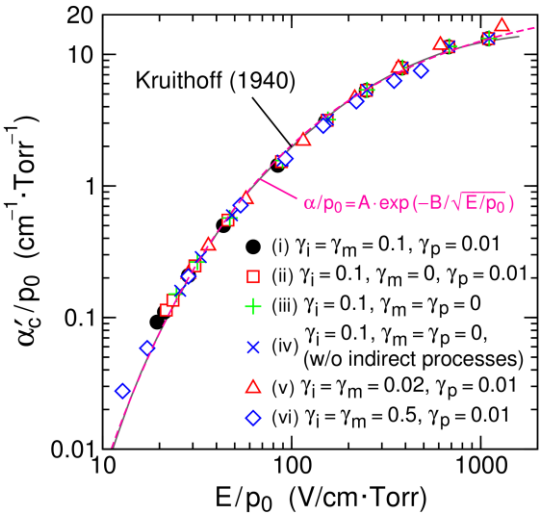

Fig. 2. Townsend's first ionisation coefficient α with various discharge conditions.

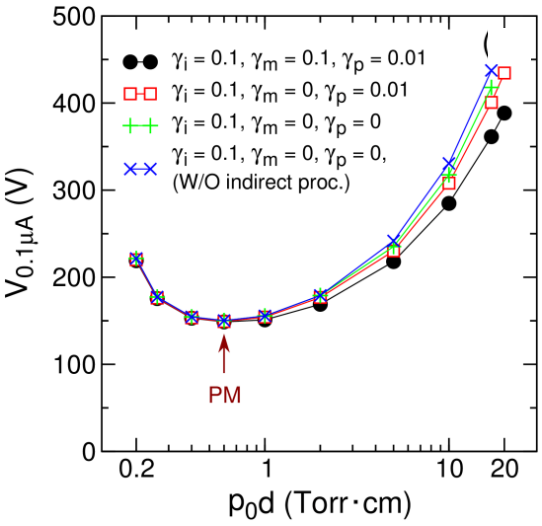

Fig. 3. Paschen's curve of Ar with various discharge conditions.

eight reaction processes are assumed. The discharge development is simulated by solving the continuity equation, the energy conservation equation for electron with the Poisson's equation.

3. RESULTS AND DISCUSSIONS

At first, to validate the present model, Townsend's first ionization coefficients αs are calculated in various conditions and compared with the measurement results of Kruithoff[3]. As shown in Fig. 2, obtained α coefficients are fairly agree with the experimental ones. As a result, the present one dimensional fluid model and swarm parameters would simulate Ar DBD discharges properly.

To find out the contributions of γ_i, γ_m, γ_p, on the breakdown voltage and other indirect ionisation processes separately, the breakdown voltages and deduced γ' are compared under the following six conditions.

(i) $\gamma_i = 0.1$, $\gamma_m = 0.1$, $\gamma_p = 0.01$
(ii) $\gamma_i = 0.1$, $\gamma_m = 0$, $\gamma_p = 0.01$
(iii) $\gamma_i = 0.1$, $\gamma_m = 0$, $\gamma_p = 0$
(iv) $\gamma_i = 0.1$, $\gamma_m = 0$, $\gamma_p = 0$
(without indirect processes)
(v) $\gamma_i = 0.02$, $\gamma_m = 0.02$, $\gamma_p = 0.01$
(vi) $\gamma_i = 0.5$, $\gamma_m = 0.5$, $\gamma_p = 0.01$

The indirect ionisation processes of cumulative ionisation and metastable-metastable collision ionisation are not considered in case (iv). By comparing cases (i)–(iv), in which a constant γ_i (= 0.1) is assumed, the contributions of γ_m, γ_p and the indirect ionisation processes (referred to as the non-ionic processes) can be evaluated. By

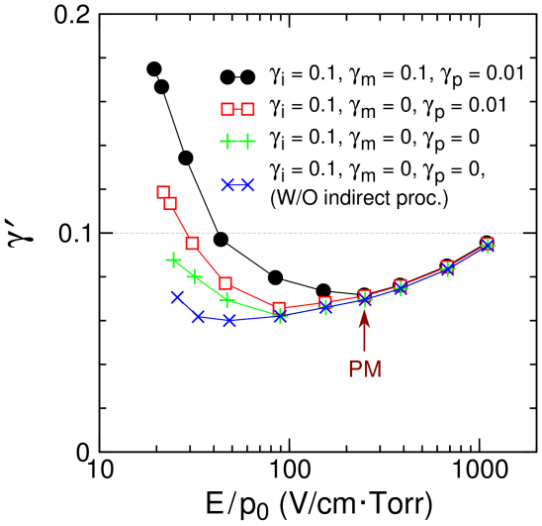

Fig. 4. Secondary ionisation coefficients with various discharge conditions.

comparing cases (i), (v) and (vi), the contributions of γ_i and γ_m can be evaluated.

Figure 3 shows the dependence of the breakdown voltage (V_{bd}) on the *pd* values (p_0d) for cases (i)–(iv). The comparison among these characteristics reveals the contributions of the non-ionic effects of γ_m, γ_p and the indirect ionisation processes. The characteristics commonly show the typical shape of Paschen's curve with the Paschen Minimum (PM) at V_{bd} ~ 150V under p_0d = 0.6 Torr·cm. Under the higher *pd* region of the Paschen's curve, V_{bd} drops as the non-ionic effects are added individually. The decrements of V_{bd} become larger as p_0d rises, suggesting that the non-ionic effects become more significant under the higher *pd* condition.

Since the non-ionic processes are all caused by

the neutral excited species (Ar^{ex} or Ar^{ms}), the drop of V_{bd} would be strongly related to the accumulation of those species. Especially, the effect of γ_m would be significant since the decrement of V_{bd} from case (ii) to case (i) is larger than other ones. This shows that the building-up of the metastable species (Ar^{ms}) during the repetitive discharge periods can affect the discharge characteristics largely not only by the gas-phase reactions but by the interactions with walls. Under the lower *pd* conditions (at or less than PM value), those species hardly accumulate in the discharge space and their effects do not appear in the characteristics of V_{bd}. Only the direct impact ionisation process and the γ_i effect can drive the discharge development in this condition.

The curves obtained in the present simulations seem to be slightly different than experimental results. In higher *pd* region, generally, breakdown voltage increases linearly with E/p_0. But in the present results, more parabolic curves are obtained. In the present model, photoionisation process is not considered. This would be one of the causes. And in the lower region, significant increase of breakdown voltage should be obtained, but in the present results, curves do not show significant increase. This may be limitation of fluid model.

In Fig. 4, the deduced γ' from the criterion are plotted against the reduced electric field (E/p_0). The PM condition corresponds to the reduced field at E/p_0 ~ 250V/cm·Torr. The higher E/p_0 represents the lower *pd* condition. When E/p_0 is higher than the PM condition, γ' approaches the given value of γ_i (= 0.1) as E/p_0 increases. The characteristics of γ' in this condition appears to be independent of the non-ionic effects as is discussed for the lower *pd* region of the Paschen's curve in Fig. 3. Under lower E/p_0, which corresponds to the higher *pd* region of the Paschen's curve, the characteristics of cases (i)–(iv) separate largely from each other.

When the non-ionic effects are absent [case (iv)], γ' tends to increase with E/p_0 except under the very low field conditions ($E/p_0 \lesssim$ 30V/cm·Torr). It remains lower than the given value of γ_i. γ' rises individually as the non-ionic effects are included. When all of the effects are included [case (i)], the relation of γ' to E/p_0 is inversed and γ' decreases with E/p_0.

Moreover, γ' exceeds the given γ_i largely under the very low field conditions. This shows that the secondary electron flux caused by the non-ionic

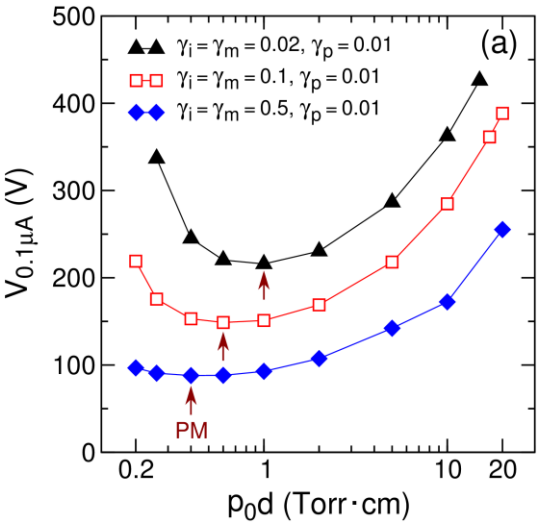

Fig. 5. Paschen's curve of Ar with various discharge conditions in different γ_i.

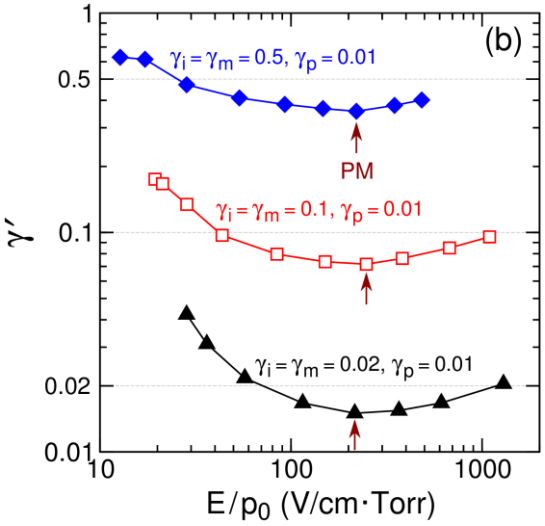

Fig. 6. Secondary ionisation coefficients with various discharge conditions in different γ_i.

processes are significantly large in addition to that caused by the ion bombardments. There are some differences between case (iii) and case (iv), suggesting that even the gas-phase reactions (indirect ionisation processes) can affect γ'. This would be related to the fact that γ' is defined in relation to α, which is essentially a parameter of gas-phase reactions. Since the non-ionic effects do not appear under PM condition, the value of γ' at PM would be an indicative parameter to estimate γ_i.

In many experiments, γ' often decreases with E/p_0[3, 4]. This tendency corresponds to the characteristics in case (i) and suggests that the effects of the non-ionic processes is actually significant. The tendency would hardly be explained without those non-ionic effects as

shown in the inversed characteristics for case (iv).

The characteristics of V_{bd} and γ' for cases (i): γ_i = 0.1, (v): γ_i = 0.02, and (vi): γ_i = 0.5 are shown in Figs. 5 and 6, respectively. The comparison among these cases reveals the contributions of γ_i. The effects of the non-ionic processes are considered in these cases.

The SEE coefficients by metastable atoms and photons are assumed to be $\gamma_m = \gamma_i$ and γ_p = 0.01, respectively. As shown in Fig. 3, the Paschen's curve changes drastically by γ_i. The PM condition moves toward the lower *pd* and V_{bd} region as γ_i rises. The decrease of V_{bd} with the increase of γ_i can be understood as that the number of the electrons yielded by SEE increases with γ_i and the discharge can develop easily.

The *pd* value decreases with the increase of γ_i so as to keep E/p_0 roughly constant. Considering that the non-ionic pro-cesses do not affect the characteristics so largely (see Fig. 3, 4), γ_i would be the most important parameter which dominantly determines the discharge characteristics. This would be consistent with that the ions' flux is the most dominant particle flux onto the electrode.

Figure 6 shows the derived γ'. It is clear that the values of γ' are dominated by γ_i as with the V_{bd} characteristics. Note that the PM condition appears under similar E/p_0 (~200–250V/cm·Torr). The non-ionic effects arisen under lower E/p_0 condition (higher *pd* condition) become relatively prominent since the γ_i effect becomes relatively smaller. The values of γ' are commonly ~ 70% of γ_i at the PM condition and tend to converge with γ_i as E/p_0 increases. As discussed with Fig. 3 and 4, the non-ionic effects do not appear under the higher E/p_0 condition around or over PM value. Supposing that the SEE flux does not depend on the external conditions such as E/p_0, the decrease of γ' from γ_i would possibly reflect the decrease of the effective secondary electron flux due to the backward scatterings. It is well understandable that γ' converges with γ_i as the *pd* value decreases since the collisions of electrons with the background gas particles would hardly occur under lower *pd* conditions. If the collision rates near the electrodes are evaluated, γ' at PM would be some indicator to estimate the actual value of γ_i.

4. CONCLUSIONS

The secondary ionization coefficient γ' is calculated using a one-dimensional fluid model simulation in order to investigate the effects of γ_i, γ_m, γ_p and the indirect ionization processes of cumulative ionization and metastable-metastable collision ionization. When the effect of the non-ionic processes are considered, the deduced γ' largely exceeds the assumed γ_i especially under the higher *pd* region of the Paschen's curve. Since the experimental characteristics of γ' which decreases with relatively lower *E/p* can hardly be explained without considering the non-ionic processes, the contributions of those processes should exist and is important in Townsend discharges under such high *pd* conditions. The contributions of those non-ionic processes tend not to appear under the lower *pd* region of the Paschen's curve and γ' tends to converge with γ_i as the reduced field increases. Therefore, by examining the value of γ' at (or around) PM, the indicative value of γ_i might be obtained.

REFERENCES

[1] G. Auday, Ph. Guillot and J. Galy panels", J. Appl. Phys. (2000), 88, 8, 4871-4874.

[2] S. Suzuki and H. Itoh, Jpn. J. Appl. Phys. (2007), 46, 3A, 1129-1136.

[3] T. Misu, M. Sugimoto, M. Goto and T. Arai: "Discharge Characteristics of MgO in Ne for Liquid Crystal Display Back-lighting Electrode", IEEJ Trans. FM, Vol.127, No.9, pp.549-552 (2007)

[4] S. Suzuki, T. Sekizawa, Y. Kashiwagi and H. Itoh: "Secondary Ionization Coefficient of MgO and Accumulated Charge", Jpn. J. Appl. Phys., Vol.50, No.10, p.106002 (2011)